

# TexSpot: 3D Texture Enhancement with Spatially-uniform Point Latent Representation

ZITENG LU\*, SSE, CUHK SZ, China and ByteDance Games, China

YUSHUANG WU\*, ByteDance Games, China

CHONGJIE YE†, FNii-Shenzhen, China and SSE, CUHK SZ, China

YUDA QIU, SSE, CUHK SZ, China

JING SHAO, SSE, CUHK SZ, China

XIAOYANG GUO, ByteDance Games, China

JIAQING ZHOU, ByteDance Games, China

TIANLEI HU, ByteDance Games, China

KUN ZHOU, Shenzhen University, China

XIAOGUANG HAN, SSE, CUHK SZ, China and FNii-Shenzhen, China

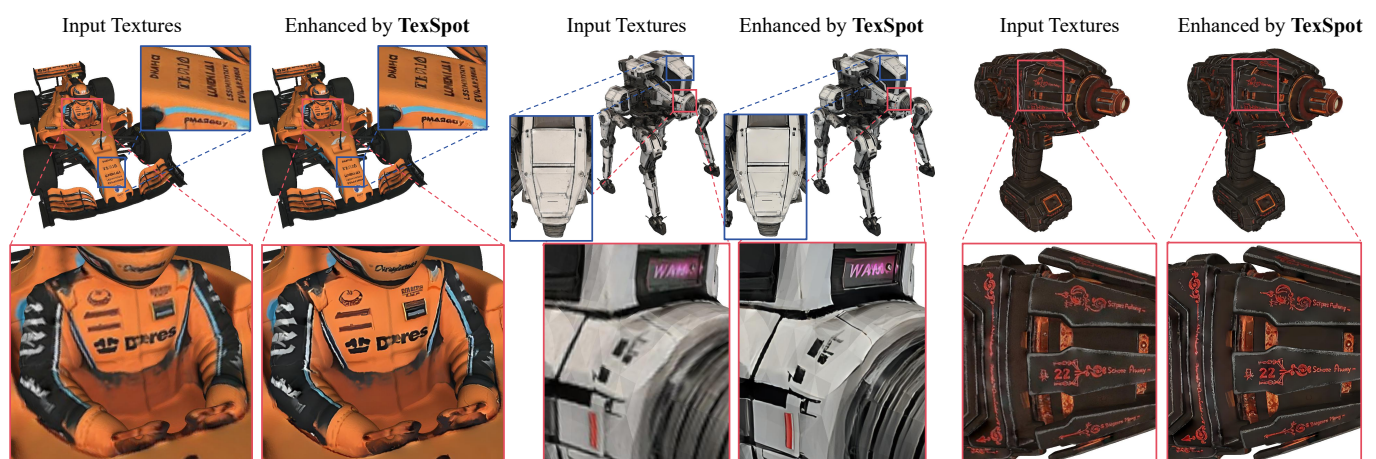


Fig. 1. Given a 3D textured model, our *TexSpot* is capable of enhancing the quality of intricate details, delivering sharper texture with fewer artifacts, even for the decent outputs generated from commercial models.

High-quality 3D texture generation remains a fundamental challenge due to the view-inconsistency inherent in current mainstream multi-view diffusion pipelines. Existing representations either rely on UV maps, which suffer from distortion during unwrapping, or point-based methods, which tightly couple texture fidelity to geometric density that limits high-resolution texture generation. To address these limitations, we introduce *TexSpot*, a diffusion-based texture enhancement framework. At its core is Texlet, a novel 3D texture representation that merges the geometric expressiveness of point-based 3D textures with the compactness of UV-based representation. Each Texlet latent vector encodes a local texture patch via a 2D encoder and is further aggregated using a 3D encoder to incorporate global shape context. A cascaded 3D-to-2D decoder reconstructs high-quality

texture patches, enabling the Texlet space learning. Leveraging this representation, we train a diffusion transformer conditioned on Texlets to refine and enhance textures produced by multi-view diffusion methods. Extensive experiments demonstrate that *TexSpot* significantly improves visual fidelity, geometric consistency, and robustness over existing state-of-the-art 3D texture generation and enhancement approaches. Project page: <https://anonymous.4open.science/w/TexSpot-page-2D91/>

CCS Concepts: • Computing methodologies → Appearance and texture representations; Neural networks.

Additional Key Words and Phrases: texture enhancement, deep neural networks

## 1 Introduction

The rapid advancement of deep learning technologies has fueled remarkable progress in the field of 3D content creation, particularly in generating high-fidelity 3D geometry [Li et al. 2025b; Team 2025; Xiang et al. 2024; Zhang et al. 2024b]. This increasing geometric fidelity further amplifies the need for photorealistic textures, making 3D texture generation a central research challenge. The ability to

\*Equal Contribution.

†Part of project lead.

Authors' Contact Information: Ziteng Lu, SSE, CUHK SZ, China and ByteDance Games, China; Yushuang Wu, ByteDance Games, China; Chongjie Ye, FNii-Shenzhen, China and SSE, CUHK SZ, China; Yuda Qiu, SSE, CUHK SZ, China; Jing Shao, SSE, CUHK SZ, China; Xiaoyang Guo, ByteDance Games, China; Jiaqing Zhou, ByteDance Games, China; Tianlei Hu, ByteDance Games, China; Kun Zhou, Shenzhen University, China; Xiaoguang Han, SSE, CUHK SZ, China and FNii-Shenzhen, China.

produce photorealistic and semantically coherent textures is paramount for applications ranging from computer graphics and virtual reality to digital twinning.

Considering the scarcity and insufficient quality of native 3D texture data, coupled with the immense computational cost of traditional texture modeling, the prevalent strategy today [Bensadoun et al. 2024; Hunyuan3D et al. 2025; Li et al. 2025a] relies on the strong priors 2D diffusion models [Blattmann et al. 2023; Labs 2024; Labs et al. 2025; Rombach et al. 2021]. This involves generating high-quality multi-view images conditioned on the input image and renders of the given white model mesh (e.g. normal maps), followed by inverse projection of color information onto the target mesh. However, this pipeline suffers from poor view-consistency among generated multi-view images, often resulting in texture mismatch or visible seams across the object’s surface. Recent efforts have explored advanced multiview-Diffusion (e.g., Hunyuan [Hunyuan3D et al. 2025], CLAY [Zhang et al. 2024b], MVPaint [Cheng et al. 2025]) and video-diffusion (e.g. SeqTex [Yuan et al. 2025]) to improve cross-view consistency. However, the projection-based paradigm remains fundamentally susceptible to self-occlusion, resulting in missing or corrupted texture regions, especially for objects with complex geometry. Our work seeks to enhance the 3D textures generated by these pipelines to improve texture quality.

The effectiveness of texture enhancement is fundamentally linked to the underlying representation. Currently, there are two mainstream representations, each with a distinct trade-off: **UV Texture Maps** (e.g. TEXGen [Yu et al. 2024] and MCMat [Zhu et al. 2024]) offer a and memory-efficient representation that enables efficient training. However, the UV unwrapping process introduces inevitable 3D-to-2D distortions and blurring—particularly for complex geometry—making high-quality UV parameterization difficult to obtain. In contrast, **Point-Based Representations** (e.g. Point-UV diffusion [Yu et al. 2023a] and TexGaussian [Xiong et al. 2025]) directly attach texture to 3D points, leveraging geometric structure for stronger spatial context. However, they inherently couple texture fidelity with point density, making high-resolution texture generation computationally expensive.



Fig. 2. The illustration of three 3D texture representation.

To address the limitations of existing 3D texture representations—namely the distortion in UV maps and the computational burden of point-based methods—we propose **TexSpot**, a texture enhancement framework with a novel 3D texture representation, **Texlet**. Texlet is designed to effectively merge the geometric expressiveness of point-based 3D textures with the compactness of UV-based representations, while introducing a spatially-uniform structure that is particularly suitable for diffusion-based learning. Specifically, Texlet is a point-attached latent representation, consisting of a set of spatial anchor points on the mesh, each associated

with a latent vector. The latent vectors are encoded globally from local texture patches, of which each patch is defined over a cluster of mesh faces obtained by grouping faces according to geometric attributes (e.g., normals). During clustering, we encourage the local flatness and boundary convexity of each cluster, which facilitates more efficient and stable encoding. As a result, the Texlet representation preserves rich geometric cues while capturing textures in a compact, group-wise latent space. Based on the Texlet representation, we develop a variational auto-encoder (VAE) with a local-global hierarchical structure for constructing the Texlet space. Each texture patch is first encoded locally by a shared 2D image encoder into a compact visual feature. These patch features are then aggregated by a 3D encoder operating on their spatial centers, thereby capturing global 3D context, to lift into the Texlet latent space. For decoding, a cascaded 3D-then-2D decoder recovers them back into texture patches, which are finally composed into the reconstructed full texture. On top of the learned Texlet space, we further train a diffusion transformer (DiT) that takes the Texlet representation of an input texture as a conditioning signal for 3D texture enhancement. We validate the effectiveness and superiority of *TexSpot* through extensive experiments, particularly focusing on the challenging task of 3D texture enhancement.

Our primary contributions are summarized as follows:

- We propose **Texlet**, a novel 3D texture representation that effectively combines the spatial consistency of 3D textures with the efficient information encoding of 2D textures, while possessing a spatially-uniform property that enables efficient diffusion learning.
- We introduce *TexSpot*, a new framework that integrates a cascaded local-global VAE to construct a robust 3D texture latent space and a latent DiT for texture enhancement based on the Texlet representation.
- We demonstrate the superiority and effectiveness of the proposed *TexSpot* framework in texture enhancement, surpassing current state-of-the-art methods.

## 2 Related Works

**Texture Generation from 3D Data.** The most straightforward approach for 3D mesh texture map synthesis involves training a generative model directly on 3D data with ground truth textures [Chang et al. 2015; Collins et al. 2022; Deitke et al. 2022]. Early methods, such as Texture Fields [Oechsle et al. 2019], learn implicit texture fields to assign a color to each pixel on the 3D surface. Texturify [Siddiqui et al. 2022] introduced a face convolution operation on the mesh surface to predict texture per face. It employs differentiable rendering combined with an adversarial loss to ensure the generated textures yield photorealistic imagery. More recently, diffusion-based texture synthesis methods, including Point-UV [Yu et al. 2023b] and TexOct [Liu et al. 2024], train a denoising network on colors of point clouds, which are subsequently mapped to a 2D UV map. Although these point-cloud-based methods achieve better 3D global consistency with the input mesh, they are typically limited by being trained on small datasets spanning only a few categories [Chang et al. 2015]. Furthermore, the reliance on discrete supervision from

3D point clouds often leads to suboptimal results compared to methods utilizing continuous signals like 2D images. Some concurrent work also explores constructing 3D latent spaces to represent mesh textures for generation or refinement [Chen et al. 2025b; Lai et al. 2025; Xiang et al. 2025; Zeng et al. 2025]. Our TexSpot is different from them in using the 2D patch as the representation unit, which has greater potential in representing fine local details and constructing the mapping between 2D image inputs and the target 3D textures.

*Texture Generation via 2D Diffusion.* To overcome the limitations of 3D-native approaches, many recent works have sought to leverage the powerful generative capabilities of 2D Text-to-Image (T2I) models to assist 3D texture generation. These methods typically render the depth map of the input 3D mesh from multiple viewpoints and use depth-conditional T2I models [Zhang et al. 2023] to synthesize RGB images, thereby performing text-conditioned texture synthesis. TEXTure [Richardson et al. 2023] and Text2Tex [Chen et al. 2023] iteratively "paint" a mesh from different views. A critical challenge in this pipeline is that errors synthesized in an early view may not be reconcilable with the geometry observed in later views, leading to multi-view inconsistency.

Many subsequent works have attempted to mitigate this inconsistency through various alignment modules. TexFusion [Cao et al. 2023] proposed a sequential interlaced multi-view sampler that interweaves texture assembling with denoising steps across different camera views. Similarly, TexGen [Huo et al. 2024] directly enforces view-consistent sampling in the RGB texture space and developed a noise resampling strategy to retain rich texture details. TexPainter [Zhang et al. 2024a] ensures multi-view consistency by blending images from different views into a common color-space texture image using weighted averaging. Paint3D [Zeng et al. 2024] contributed separate UV Inpainting and UVHD diffusion models specialized in shape-aware refinement. SeqTex [Yuan et al. 2025] introduced the use of a video diffusion model to enhance view consistency across synthesized frames.

*Image Enhancement and Super Resolution.* State-of-the-art image restoration and super-resolution (SR) methods have greatly improved visual quality. Diffusion-based models, including Diff-BIR [Lin et al. 2024], OSEDiff [Wu et al. 2024], CoSeR [Sun et al. 2024], and StableSR [Wang et al. 2024b], are particularly effective at producing highly detailed results. Nevertheless, a significant limitation of these general-purpose methods in 3D texture synthesis is their failure to maintain multi-view consistency. Tailored to this challenge, PBR-SR [Chen et al. 2025a] was recently introduced to optimize the texture of the target mesh by rendering the textured mesh into multiple image patches, then utilize 2D image priors for the super-resolution of each patch. However, since the SR prior is trained only on 2D images, the enhancement could not ensure the global consistency of the mesh texture. However, a fundamental limitation of PBR-SR is its reliance on 2D image priors to super-resolve individual rendering patches. While this approach successfully leverages the high-quality details of 2D super-resolution, it inherently lacks a mechanism to enforce global texture consistency across the

entire model. Consequently, this can result in visible seams or stylistic inconsistencies when the processed patches are assembled back onto the 3D asset.

### 3 Methodology

#### 3.1 Texture Patch Partitioning

The foundation of the whole *TexSpot* framework is the proposed Texlet representation. As illustrated in Fig. 3, each Texlet unit is processed from a texture patch, *i.e.*, a cluster of mesh faces with texture. Inspired by the design of Meshlet [Badki et al. 2020], a "good" cluster should (i) be small to have minimal distortion; (ii) be flat to avoid overshading backfaces; (iii) be near-convex and full as much as possible for more efficient encoding; and (iv) avoid self-overlap after perspective projection. We first conduct remeshing to a given mesh  $O$  via triangulation plus fine partitioning to ensure triangles are small enough. The obtained fine mesh can be represented as a dual graph  $G = (V, E)$  built over faces, where each node  $v \in V$  represents a triangle, as the initialization of a face cluster, and each edge  $e = (u, v) \in E$  connects clusters that share a boundary. For texture patch clustering, we iteratively contract the edge with minimal merging cost, defined as:

$$C = w_1 E_{\text{fit}} + w_2 E_{\text{dir}} + w_3 E_{\text{shape}} + w_4 E_{\text{count}},$$

where  $E_{\text{fit}}$  measures the flatness change computed based on the least-squares plane fitting error,  $E_{\text{dir}}$  represents surface direction coherence loss across the cluster by computing the average normal deviation angle,  $E_{\text{shape}}$  penalizes long, spindly, or concave boundaries relative to area to favor near-convex, compact clusters,  $E_{\text{count}}(p) = |N_{\max} - n(p)|$  pushes the number of triangle faces  $n(p)$  in each patch  $p$  closer to a pre-defined cluster capacity  $N_{\max}$ , and  $\{w_i\}_{i=1}^4$  are scalar weights. After iterative edge merging, we finally obtain  $N$  (very close to  $N_{\max}$ ) texture patches with small, flat, near-convex, and self-overlap-free faces in each cluster. Some visualizations are shown in Fig. 9.

#### 3.2 TexSpot VAE

Getting "good" TexSpot clusters  $z_{i=1}^N$ , we further encode each patch into compact Texlet representation. The proposed TexSpot VAE adopts a two-stage encoding: a 2D encoder for extracting rich features from local texture patches and a 3D encoder for unifying all patches at a global level. In the first encoding stage, we unwrap each texture patch onto a  $R \times R$  small image, with nearly no loss of quality, thanks to the face flatness and normal coherence in each cluster. A pretrained image encoder  $E_{2D}$  is then adopted to extract texture patch features via:

$$\phi_i = E_{2D}(z_i),$$

where  $\phi_i \in \mathbb{R}^{r \times r \times d_\phi}$  with  $r$  and  $d_\phi$  denoting the spatial and channel dimension of  $\phi_i$ , respectively. Each  $\phi_i$  is then bound with a 3-dimensional coordinate representing the 3D position of this patch feature  $p_i \in \mathbb{R}^3$ , computed as the average center of all triangles in this cluster. In the second stage, we feed the patch features  $\{\phi\}_{i=1}^N$  coupled with their positions (together with related point normals)  $\{p\}_{i=1}^N$  into a 3D encoder to get the final Texlet representation. Position embedding is performed first to project  $\{p\}_{i=1}^N$  into a higher dimension. Then an 8-layer 3D encoder compresses texture patch

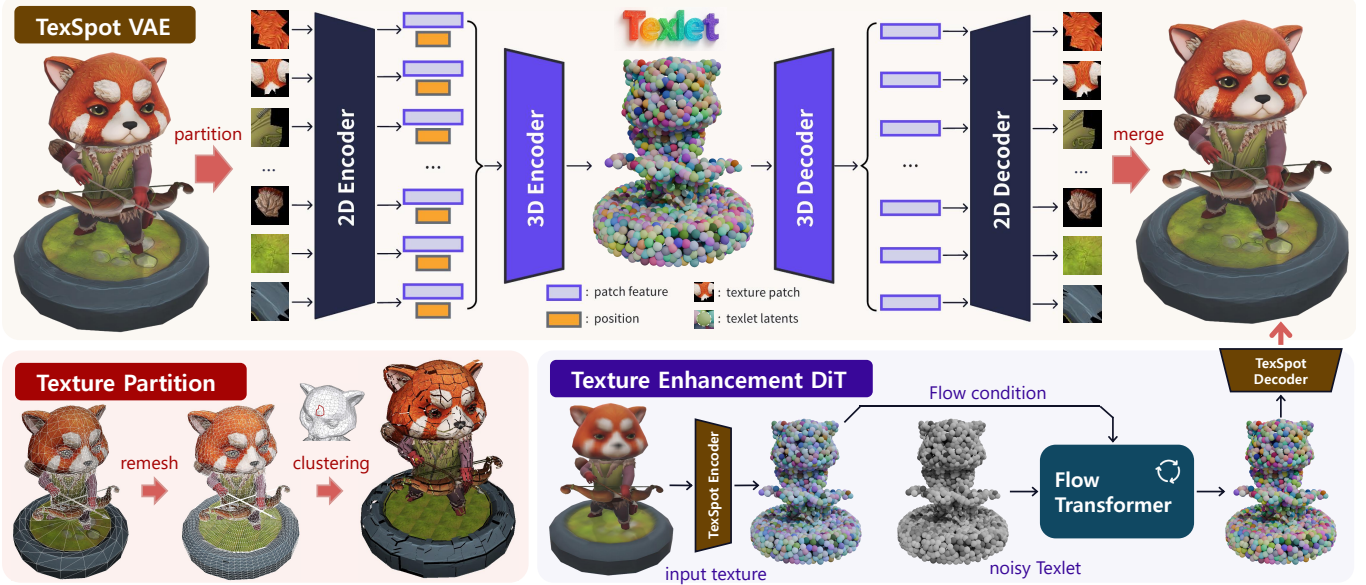


Fig. 3. The pipeline overview of *TexSpot*. It consists of (i) a texture patch partitioning that divides the surface texture into spatially-uniform small patches; (ii) a TexSpot VAE with a two-stage local-global architecture that represents all texture patches into a compact 3D latent space; and (iii) a conditional TexSpot DiT based on flow matching for texture enhancement.

features  $\{\phi\}_{i=1}^N$  together with corresponding position embedding into Texlet representations via:

$$X = E_{3D}(\{\phi_i, \text{emb}(p_i)\}_{i=1}^N),$$

where  $X \in \mathbb{R}^{N \times d}$  with  $d$ , much smaller than  $d_\phi$ , denoting the latent dimension. Cross-patch information combinations are encouraged in the 3D encoder to compress pattern-consistent/coherent texture patches into more compact Texlet representations  $X$ . The decoding follows an inverse process to the encoding. A 16-layer 3D decoder first expands  $X$  into reconstructed texture patch features:

$$\hat{\Phi} = D_{3D}(X),$$

where  $\hat{\Phi} \in \mathbb{R}^{N \times d_\phi}$  with each vector  $\hat{\phi}_i$  sharing the same feature dimension with  $\phi_i$ . Then a 2D decoder  $D_{2D}$  decodes each  $\hat{\phi}_i$  into reconstructed texture patches  $\hat{z}_i$ :

$$\hat{z}_i = D_{2D}(\hat{\phi}_i).$$

The reconstructed texture patches are finally pasted onto the mesh surface, deriving the reconstructed textured mesh  $\hat{O}$ , according to the patch partitioning and unwrapping rules of the input mesh  $O$ . The training of whole VAE employs a two-level reconstruction loss function plus a KL penalty:

$$\mathcal{L} = \alpha \mathcal{L}_{\text{patch}}(\phi_i, \hat{\phi}_i) + \beta \mathcal{L}_{\text{render}}(O, \hat{O}) + \gamma \mathcal{L}_{\text{kl}}(X),$$

where  $\mathcal{L}_{\text{patch}}$  is computed as the mean square error between each  $(\phi_i, \hat{\phi}_i)$  pair to train  $E_{3D}$  and  $D_{3D}$  for better local patch feature reconstructions,  $\mathcal{L}_{\text{render}}$  uses rendering loss for supervising the global mesh texture reconstruction,  $\mathcal{L}_{\text{kl}}$  constrains the Texlet representation  $X$  consistent with the normal distribution, and  $\alpha, \beta, \gamma$  are scalar weights.

### 3.3 Texlet-based Texture Enhancement

With a Texlet latent space, we conduct diffusion-based generative models for texture enhancement. The diffusion transformer (DiT) employs a rectified flow model [Lipman et al. 2022], where the forward process to construct the noisy Texlet  $X_t$  at the timestep  $t \in [0, 1]$  can be formulated as:

$$X_t = (1 - t)X_0 + t\epsilon,$$

i.e., the linear interpolation between a sampled  $X_0$  from the Texlet distribution and a pure noise sample  $\epsilon \in \mathbb{R}^{N \times d}$  from the normal distribution. In the backward process, we model a timestep-dependent velocity field,  $v_\theta(X_t, t) = \delta_t X_t$ , using the Texlet DiT with learnable parameters  $\theta$ , which represents the moving velocity of denoising towards the data sample.

Given an input raw texture to enhance, we first conduct texture partitioning based on the mesh geometry, and employ the pretrained encoder to represent it into Texlet  $X'$  as the condition of DiT. Therefore, DiT’s parameters  $\theta$  are optimized on a conditional flow matching (CFM) objective [Lipman et al. 2022]:

$$\mathcal{L}_{\text{cfm}}(\theta) = \mathbb{E}_{t, X_0, \epsilon} \|v_\theta(X_t, t | X') - (\epsilon - X_0)\|_2^2.$$

At the training stage, in order to encourage DiT to assign more attention on refining those “bad” patches, we re-weighting the velocity prediction loss via a weight vector  $\alpha \in [0, 1]^{N \times 1}$  with each element computed as:

$$\alpha_i = \frac{e^{\|x_i - x'_i\|_2^2}}{\sum_{i=1}^N e^{\|x_i - x'_i\|_2^2}}, i = \{1, 2, \dots, N\}$$

Besides, we take a classifier-free guidance (CFG) strategy [Ho and Salimans 2022] in training, where the condition  $X'$  is set to a null embedding with  $\rho$  probability. At the inference stage, we sample a

random noise as  $X_1$  and iteratively predict the velocity as  $t$  reduced from 1 to 0, which progressively denoises  $X_t$  and derives the final global latent prediction  $\hat{X}_0$ . The velocity  $\hat{v}_t$  with CFG at any time  $t$  is computed as:

$$\hat{v}_t = v_\theta(X_t, t|X') + \omega \cdot v_\theta(X_t, t|\emptyset),$$

where  $\omega \geq 1$  is the guidance scale determined by  $\rho$ . With the final global latent prediction  $\hat{X}_0$ , we decode it with the frozen TexSpot decoder trained at the VAE learning stage, which consists of a global 3D decoder and a local 2D decoder. The decoded texture patches are then pasted onto the input mesh according to the partition of the input texture as output.

## 4 Experiments

In this section, we evaluate the effectiveness of our *TexSpot* on the tasks of 3D texture super-resolution and 3D texture inpainting. We detail the experimental setup, evaluation metrics, and visual results.

### 4.1 Experimental Setup

*Datasets.* The scarcity of high-quality 3D texture data poses a significant challenge, as even recent datasets like TexVerse [Zhang et al. 2025] suffer from inconsistent quality. To support the training of our TexSpot VAE, we collect a dataset of 100K high-quality meshes with  $4096 \times 4096$  texture maps. To construct parid data fro texture super-resolution, we procedurally generate low-quality counterparts from these high-resolution textures using a comprehensive degradation pipeline inspired by Real-ESRGAN [Wang et al. 2021]. Specifically, low-quality counterparts are generated via a multi-stage pipeline driven by the artifacts observed in generation, rendering, multi-view fusion, camera errors, and texture storage, using down-sampling, blur, additive noise, JPEG compression, and Trellis-generated [Xiang et al. 2024] distortions. This ensures robustness to coarse, misaligned, and inconsistent textures; metrics are computed on 150 rendered views using PSNR, SSIM [Wang et al. 2004], LPIPS [Zhang et al. 2018], and FID.

*Implementation Details.* For our *TexSpot*, we first train TexSpot VAE on 8 A800 GPUs, with a batch size of 32. We then jointly fine-tune a pretrained 2D Diffusion VAE of Stable-Diffusion-1.5 [Rombach et al. 2022], with  $\alpha=1.0$ ,  $\beta=0.1$ , and  $\gamma=1e-4$ . The total training time is 7 days. For the training of texture enhancement DiT, we train the model on 8 NVIDIA H20 GPUs for 10 days, with a batch size of 8, at a learning rate of  $1e-4$  using the AdamW optimizer.

*Evaluation Metrics.* We employ some standard metrics including the Peak Signal-to-Noise Ratio (PSNR), SSIM [Wang et al. 2004], LPIPS [Zhang et al. 2018], and FID for evaluation. All metrics are computed on 150 rendered view images uniformly surrounding the centered object mesh. Higher PSNR/SSIM values and lower LPIPS/FID values indicate superior performance.

Table 1. The quantitative results of comparison with the state-of-the-art methods in the task of 3D texture super resolution. PBR-SR\* presented here is the re-implemented version by us.

Method	PSNR↑	SSIM↑	LPIPS↓	FID↓
CAMixerSR	28.36	0.8157	0.0488	54.95
DiffBIR	25.13	0.6279	0.0750	72.78
hy2.1*	28.12	0.7934	0.0624	76.58
hy2.1* w/ CAMixerSR	28.79	0.8258	0.0446	56.14
hy2.1* w/ DiffBIR	25.23	0.6065	0.0661	78.38
PBR-SR*	27.31	0.8097	0.0541	65.04
<b>Ours</b>	<b>30.04</b>	<b>0.8386</b>	<b>0.0324</b>	<b>44.02</b>

### 4.2 Results Gallery

We show the reconstructed results of our VAE in Fig. 4. The reconstructions capture the high-frequency patterns and structured patches on the ground-truth texture. More visualizations and comparisons between reconstruction results and ground truths are presented in Fig. 10.

### 4.3 Comparison

*Enhancement for 3D Texture.* Given a coarse textured 3D mesh  $LR$ , we conduct a qualitative analysis comparing our *TexSpot* with CAMixerSR [Wang et al. 2024a], DiffBIR [Lin et al. 2024], and PBR-SR [Chen et al. 2025a]. The comparison is structured into three dimensions.

First, we compare against methods that perform texture enhancement directly on the UV texture map, namely CAMixerSR and DiffBIR, using their pretrained 2D image priors (see Fig. 7, the 5-6th column). While these methods improve local texture quality, their performance is inherently limited by the complex and fragmented structure of UV layouts. For instance, the character’s eyes and the patterns on the shell exhibit visible distortions due to the lack of spatial awareness regarding the 3D geometry.

Second, we compare our approach with enhancement based on multi-view images generated by Hunyuan3D-2.1 [Hunyuan3D et al. 2025] (see Fig. 7, the 2nd column). Here, HY-2.1\* represents the original multi-view generation and enhancement pipeline. To ensure a comprehensive comparison, we also replace the default enhancement module in HY-2.1\* with CAMixerSR and DiffBIR. Although multi-view-based enhancement maintains better global consistency, it often fails to recover fine-grained local details compared to our method.

Furthermore, we evaluate against PBR-SR, which utilizes pretrained 2D priors to generate high-quality rendered patches as pseudo-ground truth (pseudo-GT) for texture optimization. Since the official code is unavailable, we re-implemented PBR-SR (denoted as PBR-SR\*) on our dataset for a fair comparison. As shown in the 7th column of Fig. 7, while PBR-SR improves local sharpness, it struggles with global consistency across different rendered views, leading to visible artifacts at patch boundaries.

In contrast, our method achieves the best overall performance in both detail recovery and global coherence, as further supported by the quantitative results in Tab. 1.

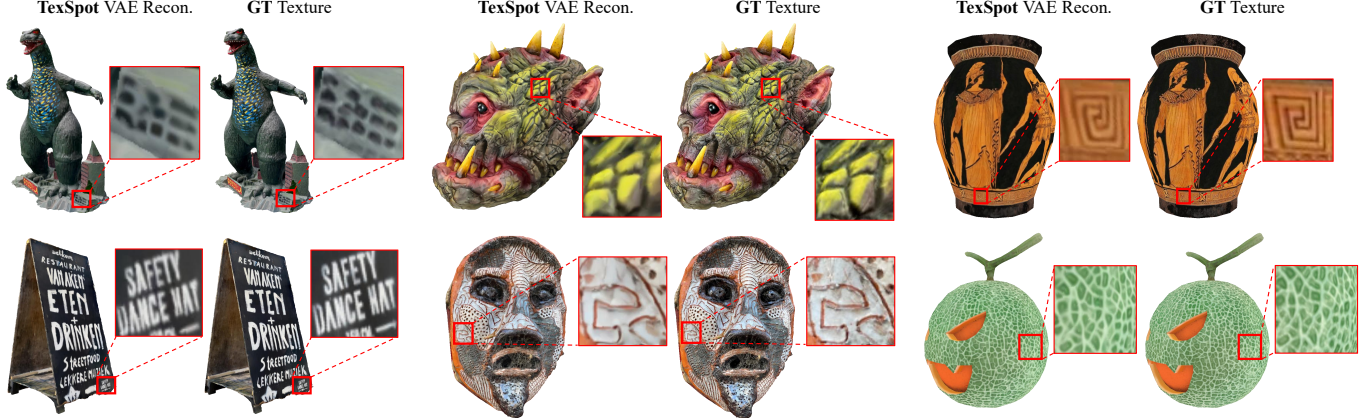
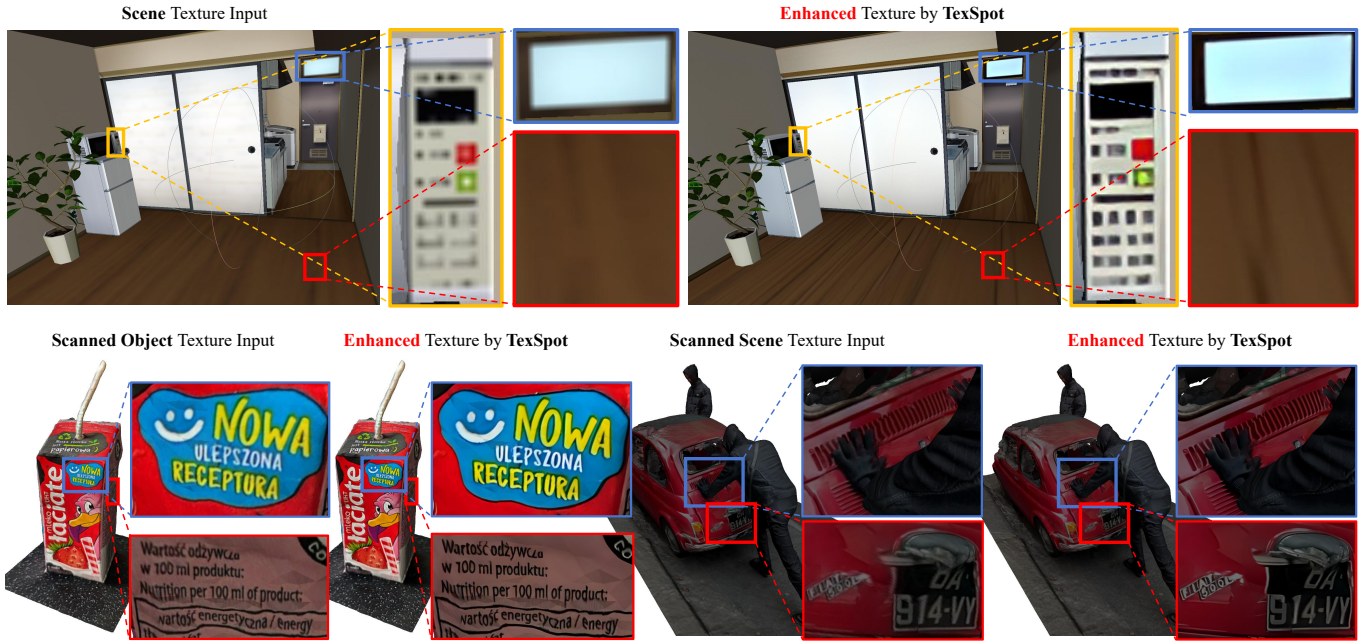


Fig. 4. Visualization of texture reconstruction results by our VAE, with comparisons with ground truth (input) textures.

Fig. 5. Texture enhancement visualization of our *TexSpot* for scanned meshes of objects or scenes.

We further show our in-the-wild testing results on enhancing textures of scanned 3D mesh in Fig. 5, as well as textures generated by powerful commercial 3D generation models [MeshyAI 2026; Tripo3d 2026] in Fig. 6. Our *TexSpot* is capable to enhance the quality of intricate details, delivering sharper texture with fewer artifacts, even for the decent outputs scanned from real world and generated from commercial models. More results are shown in the supplementary materials.

#### 4.4 Ablation Study

We examine the effectiveness of each key component in our pipeline configuration.

Table 2. Ablation results of different variants of our *TexSpot* on the patch number choice and the SD VAE implementation.

Ver- sion	Conv		# Patches			Results	
	NFNet	SD-VAE	2048	4096	8192	PSNR↑	SSIM↑
(a)	✓				✓	25.73	0.7247
(b)		✓	✓			26.04	0.7769
(c)		✓		✓		30.50	0.8809
(d)		✓			✓	34.21	<b>0.9320</b>

*Number of Texlet Patches per Mesh.* The number  $N$  of Texlet patches significantly influences the capacity of texture modeling. We ablate this design choice by testing  $N$  values of: 2048, 4096, and

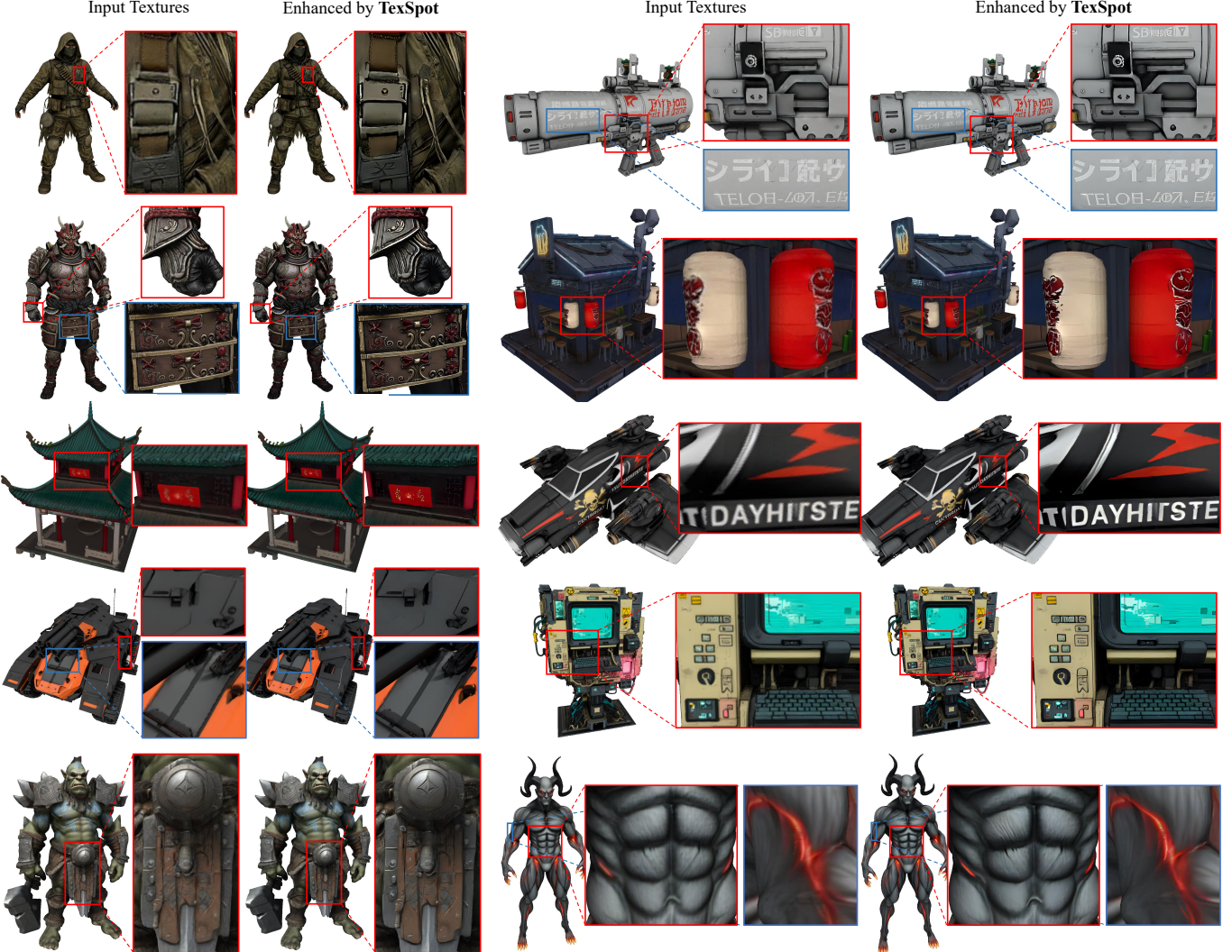


Fig. 6. Texture Enhancement result for generated textured 3D mesh. We adopt Meshy-6 [MeshyAI 2026] and Tripo3D-3.0 [Tripo3d 2026] to generate the coarse texture and use our model for enhancement. Despite the decent texture quality produced by commercial models, our *TexSpot* consistently improves the quality of intricate details, delivering sharper outputs with fewer artifacts. Please zoom in for a more detailed comparison of the textures.

8192. As shown in Tab. 2 and Fig. 8 (b,c,d), when  $N$  reaches 8192, the reconstruction quality is comparable to the corresponding ground truth. In our experiments, further increasing the number of Texlet patches does not yield significant performance improvements for the VAE.

*Effectiveness of SD VAE.* We conduct an ablation study to investigate the necessity of incorporating the SD VAE. Specifically, we train a baseline model where the texture patch is compressed into the texture latent using a dedicated convolution module NFNet. The results shown in Fig. 8 and Tab. 2 ((a) v.s. (d)) demonstrate that leveraging the powerful 2D image prior from the SD VAE significantly enhances the model’s generalization capability, enabling high-quality modeling for a wide variety of complex texture patches.

## 5 Conclusion and Limitation

In this work, we tackled the persistent challenge of high-quality 3D texture generation under view-inconsistent multi-view diffusion pipelines and limitations of existing texture representations. We introduced *TexSpot*, a diffusion-based texture enhancement framework built upon Texlet, a novel 3D texture representation that combines the geometric expressiveness of point-based methods with the compactness of UV-based representations. By encoding local texture patches with a 2D encoder, aggregating them via a 3D encoder conditioned on spatial layout, and reconstructing them through a cascaded 3D-to-2D decoder, *TexSpot* learns a structured latent space tailored for 3D textures. On top of this representation, we trained

a diffusion transformer conditioned on Texlets to refine and enhance textures generated by multi-view diffusion methods. Extensive experiments show that *TexSpot* consistently improves visual fidelity, geometric consistency, and robustness over state-of-the-art 3D texture generation and enhancement approaches, particularly in challenging regions affected by view inconsistency and complex geometry. Looking forward, the Texlet latent space provides a principled foundation for more advanced operations, such as controllable texture editing, style transfer across shapes, and jointly learned geometry–texture generative models. We believe *TexSpot* opens up a promising direction for structured, representation-aware 3D texture modeling in modern generative pipelines.

*Limitations.* Our approach still has several limitations. The Texlet representation depends on geometry-aware clustering, which can be unstable on highly noisy or very low-quality meshes and may degrade reconstruction in such cases. In addition, because *TexSpot* operates as a post-hoc enhancement stage, the enhancement effect can be influenced by the quality of the initial textures; severely missing or hallucinated content cannot always be fully corrected. Exploring more efficient Texlet construction and tighter integration with upstream generation models is an important direction for future work. Besides, using the Texlet representation for image-based generative learning is also one of our future work.

## References

Abhishek Badki, Orazio Gallo, Jan Kautz, and Pradeep Sen. 2020. Meshlet priors for 3d mesh reconstruction. 2849–2858.

Raphael Bensadoun, Yanir Kleiman, Idan Azuri, Omri Harosh, Andrea Vedaldi, Natalia Neverova, and Oran Gafni. 2024. Meta 3d texturegen: Fast and consistent texture generation for 3d objects. *arXiv preprint arXiv:2407.02430* (2024).

Andreas Blattmann, Tim Dockhorn, Suniti Kulal, Daniel Mendelovich, Maciej Kilian, Dominik Lorenz, Yam Levi, Zion English, Vikram Voleti, Adam Letts, et al. 2023. Stable video diffusion: Scaling latent video diffusion models to large datasets. *arXiv preprint arXiv:2311.15127* (2023).

Tianshi Cao, Karsten Kreis, Sanja Fidler, Nicholas Sharp, and Kangxue Yin. 2023. Texfusion: Synthesizing 3d textures with text-guided image diffusion models. In *Proceedings of the IEEE/CVF international conference on computer vision*. 4169–4181.

Angel X Chang, Thomas Funkhouser, Leonidas Guibas, Pat Hanrahan, Qixing Huang, Zimo Li, Silvio Savarese, Manolis Savva, Shuran Song, Hao Su, et al. 2015. Shapenet: An information-rich 3d model repository. *arXiv preprint arXiv:1512.03012* (2015).

Chia-Hao Chen, Zi-Xin Zou, Yan-Pei Cao, Ze Yuan, Guan Luo, Xiaojuan Qi, Ding Liang, Song-Hai Zhang, and Yuan-Chen Guo. 2025b. LaFiTe: A Generative Latent Field for 3D Native Texturing. *arXiv preprint arXiv:2512.04786* (2025).

Dave Zhenyu Chen, Yawar Siddiqui, Hsin-Ying Lee, Sergey Tulyakov, and Matthias Nießner. 2023. Text2tex: Text-driven texture synthesis via diffusion models. In *Proceedings of the IEEE/CVF international conference on computer vision*. 18558–18568.

Yujin Chen, Yinyu Nie, Benjamin Ummenhofer, Reiner Birlk, Michael Paulitsch, and Matthias Nießner. 2025a. PBR-SR: Mesh PBR Texture Super Resolution from 2D Image Priors. *arXiv preprint arXiv:2506.02846* (2025).

Wei Cheng, Juncheng Mu, Xianfang Zeng, Xin Chen, Anqi Pang, Chi Zhang, Zhibin Wang, Bin Fu, Gang Yu, Ziwei Liu, et al. 2025. Mpavpt: Synchronized multi-view diffusion for painting anything 3d. 585–594.

Jasmine Collins, Shubham Goel, Kenan Deng, Achleshwar Luthra, Leon Xu, Erhan Gundogdu, Xi Zhang, Tomas F Yago Vicente, Thomas Dideriksen, Himanshu Arora, Matthieu Guillaumin, and Jitendra Malik. 2022. ABO: Dataset and Benchmarks for Real-World 3D Object Understanding. *CVPR* (2022).

Matt Deitke, Dustin Schwenk, Jordi Salvador, Luca Wehrs, Oscar Michel, Eli Vandenberg, Ludwig Schmidt, Kiana Ehsani, Aniruddha Kembhavi, and Ali Farhadi. 2022. Objaverse: A Universe of Annotated 3D Objects. *arXiv preprint arXiv:2212.08051* (2022).

Jonathan Ho and Tim Salimans. 2022. Classifier-free diffusion guidance. *arXiv preprint arXiv:2207.12598* (2022).

Team Hunyuan3D, Shuhui Yang, Mingxin Yang, Yifei Feng, Xin Huang, Sheng Zhang, Zebin He, Di Luo, Haolin Liu, Yunfei Zhao, et al. 2025. Hunyuan3D 2.1: From Images to High-Fidelity 3D Assets with Production-Ready PBR Material. *arXiv preprint arXiv:2506.15442* (2025).

Dong Huo, Zixin Guo, Xinxin Zuo, Zhihao Shi, Juwei Lu, Peng Dai, Songcen Xu, Li Cheng, and Yee-Hong Yang. 2024. Texgen: Text-guided 3d texture generation with multi-view sampling and resampling. In *European Conference on Computer Vision*. Springer, 352–368.

Black Forest Labs. 2024. FLUX. <https://github.com/black-forest-labs/flux>.

Black Forest Labs, Stephen Batifol, Andreas Blattmann, Frederic Boesel, Saksham Consul, Cyril Diagne, Tim Dockhorn, Jack English, Zion English, Patrick Esser, Sumith Kulal, Kyle Lacey, Yam Levi, Cheng Li, Dominik Lorenz, Jonas Müller, Dustin Podell, Robin Rombach, Harry Saini, Axel Sauer, and Luke Smith. 2025. FLUX.1 Kontext: Flow Matching for In-Context Image Generation and Editing in Latent Space. *arXiv:2506.15742 [cs.GR]* <https://arxiv.org/abs/2506.15742>

Zeqiang Lai, Yunfei Zhao, Zibo Zhao, Xin Yang, Xin Huang, Jingwei Huang, Xiangyu Yue, and Chunhao Guo. 2025. NaTex: Seamless Texture Generation as Latent Color Diffusion. *arXiv preprint arXiv:2511.16317* (2025).

Weiyu Li, Xuanyang Zhang, Zheng Sun, Di Qi, Hao Li, Wei Cheng, Weiwei Cai, Shihao Wu, Jiarui Liu, Zihao Wang, et al. 2025a. Step1X-3D: Towards High-Fidelity and Controllable Generation of Textured 3D Assets. *arXiv preprint arXiv:2505.07747* (2025).

Yangguang Li, Zi-Xin Zou, Zexiang Liu, Dehu Wang, Yuan Liang, Zhipeng Yu, Xingchao Liu, Yuan-Chen Guo, Ding Liang, Wanli Ouyang, et al. 2025b. TripoSG: High-Fidelity 3D Shape Synthesis using Large-Scale Rectified Flow Models. *arXiv preprint arXiv:2502.06608* (2025).

Xinqi Lin, Jingwen He, Ziyan Chen, Zhaoyang Lyu, Bo Dai, Fanghua Yu, Yu Qiao, Wanli Ouyang, and Chao Dong. 2024. Diffbir: Toward blind image restoration with generative diffusion prior. In *European conference on computer vision*. Springer, 430–448.

Yaron Lipman, Ricky TQ Chen, Heli Ben-Hamu, Maximilian Nickel, and Matt Le. 2022. Flow matching for generative modeling. *arXiv preprint arXiv:2210.02747* (2022).

Jialun Liu, Chenming Wu, Xinqi Liu, Xing Liu, Jinbo Wu, Haotian Peng, Chen Zhao, Haocheng Feng, Jingtuo Liu, and Errui Ding. 2024. Texoct: Generating textures of 3d models with octree-based diffusion. In *Proceedings of the IEEE/CVF Conference on Computer Vision and Pattern Recognition*. 4284–4293.

MeshyAI. 2026. <https://www.meshy.ai>

Michael Oechsle, Lars Mescheder, Michael Niemeyer, Thilo Strauss, and Andreas Geiger. 2019. Texture Fields: Learning Texture Representations in Function Space. In *Proceedings IEEE International Conf. on Computer Vision (ICCV)*.

Elad Richardson, Gal Metzger, Yuval Alaluf, Raja Giryes, and Daniel Cohen-Or. 2023. Texture: Text-guided texturing of 3d shapes. In *ACM SIGGRAPH 2023 conference proceedings*. 1–11.

Robin Rombach, Andreas Blattmann, Dominik Lorenz, Patrick Esser, and Björn Ommer. 2021. High-Resolution Image Synthesis with Latent Diffusion Models. *arXiv:2112.10752 [cs.CV]*

Robin Rombach, Andreas Blattmann, Dominik Lorenz, Patrick Esser, and Björn Ommer. 2022. High-resolution image synthesis with latent diffusion models. In *Proceedings of the IEEE/CVF conference on computer vision and pattern recognition*. 10684–10695.

Yawar Siddiqui, Justus Thies, Fangchang Ma, Qi Shan, Matthias Nießner, and Angela Dai. 2022. Texturify: Generating textures on 3d shape surfaces. In *European Conference on Computer Vision*. Springer, 72–88.

Haoze Sun, Wenbo Li, Jianzhuang Liu, Haoyu Chen, Renjing Pei, Xueyi Zou, Youliang Yan, and Yujiu Yang. 2024. CoSeR: Bridging Image and Language for Cognitive Super-Resolution. In *Proceedings of the IEEE/CVF Conference on Computer Vision and Pattern Recognition (CVPR)*. 25868–25878.

Tencent Hunyuan3D Team. 2025. Hunyuan3D 2.1: From Images to High-Fidelity 3D Assets with Production-Ready PBR Material. *arXiv:2506.15442 [cs.CV]*

Tripo3d. 2026. <https://www.tripo3d.ai>

Jianyi Wang, Zongsheng Yue, Shangchen Zhou, Kelvin C.K. Chan, and Chen Change Loy. 2024b. Exploiting Diffusion Prior for Real-World Image Super-Resolution. (2024).

Xiantao Wang, Liangbin Xie, Chao Dong, and Ying Shan. 2021. Real-esrgan: Training real-world blind super-resolution with pure synthetic data. In *Proceedings of the IEEE/CVF international conference on computer vision*. 1905–1914.

Yan Wang, Yi Liu, Shijie Zhao, Junlin Li, and Li Zhang. 2024a. CAMixerSR: Only Details Need More “Attention”. *arXiv preprint arXiv:2402.19289* (2024).

Zhou Wang, Alan C Bovik, Hamid R Sheikh, and Eero P Simoncelli. 2004. Image quality assessment: from error visibility to structural similarity. 13, 4 (2004), 600–612.

Rongyuan Wu, Lingchen Sun, Zhiyuan Ma, and Lei Zhang. 2024. One-step effective diffusion network for real-world image super-resolution. *Advances in Neural Information Processing Systems* 37 (2024), 92529–92553.

Jianfeng Xiang, Xiaoxue Chen, Sicheng Xu, Ruicheng Wang, Zelong Lv, Yu Deng, Hongyuan Zhu, Yue Dong, Hao Zhao, Nicholas Jing Yuan, et al. 2025. Native and Compact Structured Latents for 3D Generation. *arXiv preprint arXiv:2512.14692* (2025).

Jianfeng Xiang, Zelong Lv, Sicheng Xu, Yu Deng, Ruicheng Wang, Bowen Zhang, Dong Chen, Xin Tong, and Jiaolong Yang. 2024. Structured 3D Latents for Scalable and Versatile 3D Generation. *arXiv preprint arXiv:2412.01506* (2024).

Bojun Xiong, Jialun Liu, Jiakui Hu, Chennming Wu, Jinbo Wu, Xing Liu, Chen Zhao, Errui Ding, and Zhouhui Lian. 2025. Texgaussian: Generating high-quality pbr material via octree-based 3d gaussian splatting. 551–561.

Xin Yu, Peng Dai, Wenbo Li, Lan Ma, Zhengzhe Liu, and Xiaojuan Qi. 2023a. Texture generation on 3d meshes with point-uv diffusion. 4206–4216.

Xin Yu, Peng Dai, Wenbo Li, Lan Ma, Zhengzhe Liu, and Xiaojuan Qi. 2023b. Texture generation on 3d meshes with point-uv diffusion. In *Proceedings of the IEEE/CVF International Conference on Computer Vision*. 4206–4216.

Xin Yu, Ze Yuan, Yuan-Chen Guo, Ying-Tian Liu, Jianhui Liu, Yangguang Li, Yan-Pei Cao, Ding Liang, and Xiaojuan Qi. 2024. Texgen: a generative diffusion model for mesh textures. *ACM Transactions on Graphics* 43, 6 (2024), 1–14.

Ze Yuan, Xin Yu, Yangtian Sun, Yuan-Chen Guo, Yan-Pei Cao, Ding Liang, and Xiaojuan Qi. 2025. SeqTex: Generate Mesh Textures in Video Sequence. *arXiv preprint arXiv:2507.04285* (2025).

Xianfang Zeng, Xin Chen, Zhongqi Qi, Wen Liu, Zibo Zhao, Zhibin Wang, Bin Fu, Yong Liu, and Gang Yu. 2024. Paint3d: Paint anything 3d with lighting-less texture diffusion models. In *Proceedings of the IEEE/CVF conference on computer vision and pattern recognition*. 4252–4262.

Yifei Zeng, Yajie Bao, Jiachen Qian, Shuang Wu, Youtian Lin, Hao Zhu, Buyu Li, Feihu Zhang, Xun Cao, and Yao Yao. 2025. TEXTRIX: Latent Attribute Grid for Native Texture Generation and Beyond. *arXiv preprint arXiv:2512.02993* (2025).

Hongkun Zhang, Zherong Pan, Congyi Zhang, Lifeng Zhu, and Xifeng Gao. 2024a. Texpainter: Generative mesh texturing with multi-view consistency. In *Acm siggraph 2024 conference papers*. 1–11.

Lvmin Zhang, Anyi Rao, and Maneesh Agrawala. 2023. Adding Conditional Control to Text-to-Image Diffusion Models.

Longwen Zhang, Ziyu Wang, Qixuan Zhang, Qiwei Qiu, Anqi Pang, Haoran Jiang, Wei Yang, Lan Xu, and Jingyi Yu. 2024b. CLAY: A Controllable Large-scale Generative Model for Creating High-quality 3D Assets. *arXiv preprint arXiv:2406.13897* (2024).

Richard Zhang, Phillip Isola, Alexei A Efros, Eli Shechtman, and Oliver Wang. 2018. The unreasonable effectiveness of deep features as a perceptual metric. 586–595.

Yibo Zhang, Li Zhang, Rui Ma, and Nan Cao. 2025. TexVerse: A Universe of 3D Objects with High-Resolution Textures. *arXiv:2508.10868 [cs.CV]* <https://arxiv.org/abs/2508.10868>

Shenhai Zhu, Lingteng Qiu, Xiaodong Gu, Zhengyi Zhao, Chao Xu, Yuxiao He, Zhe Li, Xiaoguang Han, Yao Yao, Xun Cao, et al. 2024. Mcmat: Multiview-consistent and physically accurate pbr material generation. *arXiv preprint arXiv:2412.14148* (2024).



Fig. 7. The qualitative results of comparison with the state-of-the-art methods in the task of 3D texture super resolution. Our *TexSpot* achieves the best performance in texture quality and global consistency. PBR-SR presented here is the re-implemented version by us.



Fig. 8. The reconstruction results of VAE under different configurations of Texlet quantities. (a) represents baseline using NFNet. For (b)-(d),  $N=2048$ ,  $4096$ , and  $8192$ , respectively. When  $N$  reaches  $8192$ , the reconstruction quality is comparable to the corresponding ground truth.

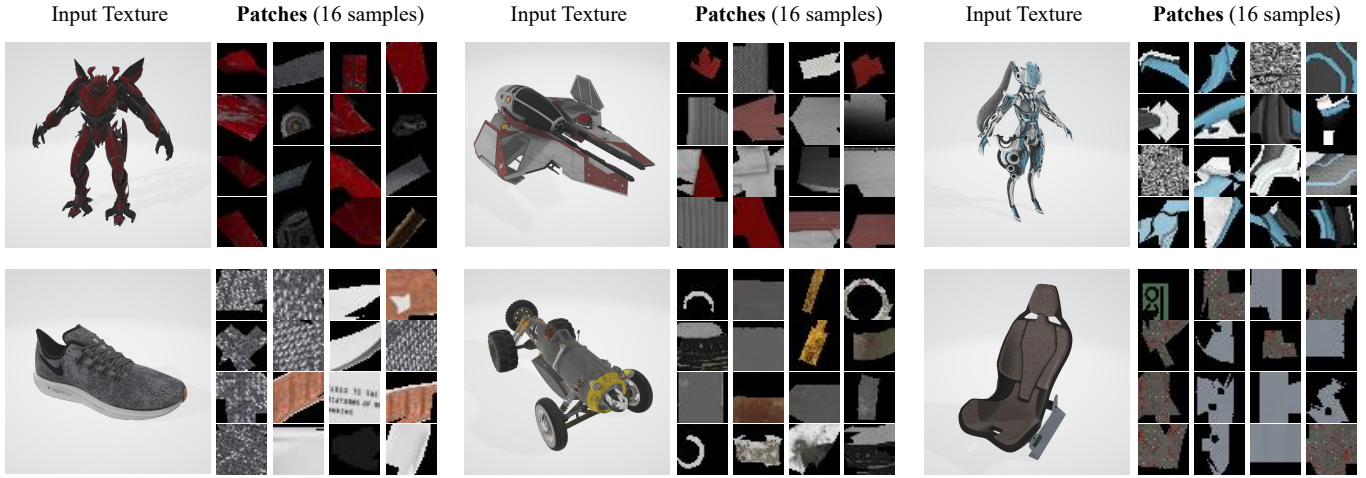


Fig. 9. Visualization of mesh textures in training data, and 16 samples of image patches produced by TexSpot.



Fig. 10. The reconstructed results of our VAE. The reconstructions capture the high-frequency patterns and structured patches on the ground-truth texture. Better zoom in to observe fine details in the texture reconstruction results.